Chemistry Africa (2024) 7:3903–3915
https://doi.org/10.1007/s42250-024-00974-7

ORIGINAL ARTICLE

High Performance Activated Carbon Based on Date Palm Fibers for Cu^{2+} Removal in Water

Amina Soudani[1] · Leila Youcef[2] · Soufiane Youcef[3] · Sara Elbahi[4] · Khaoula Toumi[5] · Guergazi Saadia[2] · Amane Sahli[6] · Nafissa Soudani[7]

Received: 6 December 2023 / Accepted: 15 April 2024 / Published online: 21 May 2024

Abstract

The aim of the present study was to produce a date palm fibers-based activated carbon (DPFAC) using phosphoric acid as an activating agent. DPFAC has been studied as a promising adsorbent for the removal of copper ions from synthetic solutions. DPFAC characterization performed by Fourier Transform Infrared Spectroscopy (FTIR), Scanning Electron Microscopy (SEM) and Brunauer–Emmett–Teller (BET) indicated that DPFAC morphology and texture were well-developed with various surface bonds and high specific surface area and average pore diameter (834.79 m^2/g, 17.48 Å, repectively). The results of the kinetic adsorption test showed that DPFAC achieved high Cu^{2+} removal efficiency (94.47%) at equilibrium time (60 min). The kinetic data fitted perfectly with the pseudo-second-order model. Three intra-particle diffusion steps are implicated in the adsorption of Cu^{2+}. Solution pH has a considerable influence on Cu^{2+} removal efficiency. The isotherm models (Langmuir, Freundlich, Redlich-Peterson and Sips) showed an adequate fit to the experimental points, proving that the transfer of Cu^{2+} onto the DPFAC surface was favorable. Langmuir model provided the best fit, with a maximum adsorption capacity of 48.59 mg/g. The thermodynamic study performed between 20°C and 50°C confirmed that the adsorption process is spontaneous and endothermic, and may involve physisorption enhanced by chemisorption. Based on tested reaction parameters, it is clear that the use of date palm fibers for the preparation of DPFAC was highly effective in removing copper ions from wastewater.

Keywords Date palm fibers · Activated carbon · Copper · Adsorption · Mechanisms

✉ Amina Soudani
amina.soudani@univ-biskra.dz

✉ Leila Youcef
l.youcef@univ-biskra.dz

[1] Industrial Chemistry Department, Research Laboratory in Subterranean and Surface Hydraulics, Mohamed Khider University, Biskra, Algeria

[2] Civil Engineering and Hydraulic Department, Research Laboratory in Subterranean and Surface Hydraulics, Mohamed Khider University, Biskra, Algeria

[3] Geotechnics and Hydraulics Department, Faculty of Civil Engineering, USTHB University, Algiers, Research Laboratory in Subterranean and Surface Hydraulics, Mohamed Khider University, Biskra, Algeria

[4] Civil Engineering and Hydraulic Department, Mohamed Khider University, Biskra, Algeria

[5] Higher School of Agriculture of Kef (ESAK), LR14AGR04: Support for the Sustainability of Agricultural Production Systems in the North West Region, University of Jendouba, Le Kef, Tunisia

[6] Department of Fuel, Nuclear Research Center of Draria CRND, Laboratory of Earthquake Engineering and Structural Dynamics, National Polytechnic School, Algiers, Algeria

[7] Department of Agricultural Sciences, Laboratory of Promotion of Innovation in Agriculture in Arid Regions (PIAAR), Mohamed Khider University, Biskra, Algeria

1 Introduction

Water contamination caused by heavy metals in the wastewater from industrial, urban, and agricultural sources is a major environmental problem, and a serious challenge throughout the world [1–3]. Since heavy metals are present in surface water and groundwater, they cause several serious health issues that affect animals, plants, and humans [4].

Heavy metals can bind covalently to organic groups to form lipophilic compounds or ions. In the human body, they cross the cell membrane and can penetrate the cell. These metallic compounds cause toxic effects when they interact with cell organelles [4]. When consumed in excess levels, these heavy metals accumulate in the intracellular or extracellular space of the organs of the body and become lethal [5]. These include copper ions, which are recognized as being vital to a variety of organisms. Therefore, copper (Cu) is widely considered being toxic when this metal ion exceeds in drinking water the level of 2 mg/L [6, 7]. A wide range of health symptoms, such as renal lesions, high fevers, hemolysis, and stomach problems could be linked to water contamination with copper ions [8]. To face this problem, treatment of polluted water was regarded as necessary in order to limit the risk of pollution by heavy metals. A number of techniques focusing on physicochemical approaches have been implemented. Including coagulation-flocculation, precipitation, advanced oxidation technology, membrane treatment methods [2, 9] and biological methods [4].

In recent years, adsorption has emerged as a promising alternative to conventional methods for the treatment of wastewater containing high levels of heavy metals. **T**his separation process has been considered efficient due to the low energy requirement and cost of operation [10, 11].The most appropriate adsorbents for removing inorganic contaminants from wastewater are selected based on technical, economic and performance considerations [12, 13]. Consequently, activated carbons derived from agricultural residues generated a considerable amount of investment in the treatment of contaminated water. These materials are considered as environmentally sustainable and cost-effective [14–16]. Chemical activation using phosphoric acid (H_3PO_4) to enhance the physicochemical properties of biomass is widely reported [16–18]. Moreover, H_3PO_4 is eco-friendly as it is non-polluting, easy to recover and can be recycled back into the process [16, 19–21]. Lignocellulosic material acid phosphoric-impregnated then carbonized disply high surface area and regular pores [22, 23]. Phosphoric acid activation leads to bond weakening and the formation of cross-linked structure [24]. Phosphoric acid activated adsorbents can be recycled and have low toxicity [18]. Use of tell activated carbons has proven high ability to adsorb heavy metal ions from water [17, 20, 21, 25, 26].

Date palm is a native tree of the North African countries [23, 27]. In Algeria, the date palm is the driving force behind sustainable development and the preservation of life in the desert given its benefits. The benefits include fruit and its uses, the palms for baskets and carpets, the fibers for ropes, trunks and palms for roofs and house foundations, and all these residues can be used as fuel [28].

Date palm fibers constitute a portion of the large quantities of waste generated by date palms pruned each year to cut branches and fibers [29, 30]. Date palm fibers (DPF) have been considered basic biomass for the preparation of efficient adsorbents for heavy metal removal [31]. The use of DPF washed and then dried at 105 °C by Al-Ghamdi et al.[32] resulted in a maximum Langmuir capacity of around 54.57 mg/g for cadmium. Amin et al. [33] reported 25.25 mg/g for copper removal. Hikmat et al. [34] used DPF washed then dried at 110 °C and resulting in a lead adsorption capacity of around 22.95 mg/g. Basheer et al. [35] prepared a DPF activated carbon using KOH. This activated carbon provided a very significant adsorption capacity (1013 mg/g) when tested in the removal of Al^{3+}. Melliti et al. [36] reported that DPF activated with $ZnCl_2$ resulted in a maximum adsorption capacity of 25.05 mg/g and 29.86 mg/g for Cu^{2+} and Pb^{2+}, respectively.

To the best of our knowledge, from previously published research, the use of date palm fibers from the palm trunk as activated carbon obtained by using phosphoric acid to remove heavy metals in solutions has not been investigated. Consequently, the present study aimed to synthesize activated carbon from date palm fibers using H_3PO_4 as an agent of activation to produce an adsorbent with highly developed textural and morphological properties. The synthesized activated carbon was tested as an adsorbent for copper ions from aqueous solutions. The effects of various reaction parameters, including contact time, initial solution pH, initial copper ions concentration, and temperature, were investigated and results were discussed. The results and discussion provide insights into the effectiveness of DPFAC in adsorbing copper ions from contaminated water.

2 Material and Methods

2.1 Reagents and Chemicals Used

A solution of Cu^{2+} (1000 mg /L) was freshly obtained by dissolution of an analytical grade ($CuSO_4$, $5H_2O$) with 99% purity in distilled water. Dilutions of this solution were performed for the required concentration. The pH of the solutions was adjusted to the required value using 0.1 M solutions of sodium hydroxide or hydrochloric acid. Chemical activation was carried out using phosphoric acid H_3PO_4 (50%).

2.2 Preparation of the Adsorbent

Date palm fibers (DPF) were collected from the palm trunk in October during the cleaning process of the date palm trees of Deglet Nour located in Sidi Okba, commune of Biskra (Southeastern Algeria). The adsorbent was produced using the process shown in Fig. 1. Formoste, the DPF were carefully cleaned of any impurities that might have attached to them, and then sun-dried. Following this operation, the material was cut into small pieces. Then 60 g of DPF was impregnated in 100 mL of phosphoric acid solution (H_3PO_4, 50%) for 24 h [22]. The mixture was transferred to a rotary evaporator and stirred at 60 rpm under a temperature of 110 °C for 2 h. Then, the mixture was filtered and the resulting material was placed in the oven to dry for 20 min at 110°C. This operation was followed by pyrolysis at 400°C for 2 h under oxygen-limited conditions in a muffle furnace. The sample was neutralised using soxhlet extraction and distilled water. Next, the material was placed in beakers containing distilled water and exposed in an ultrasound processor (Bioblock scientific ultrasonics 88,155) for approximately 30 min at a working frequency of 35 kHz. Following this operation, the product was dried for 24 h at 110°C then milled with mortal until obtaining a material with a particle size between 0.1 and 0.25 mm. The resulting date palm fibers activated carbon was designated DPFAC.

2.3 Characterization of the Prepared Adsorbent

The FTIR (Fourier Transform Infra-Red) spectrum of DPFAC was obtained using a Perkin Elmer Spectrum Two instrument. SEM (Scanning Electron Microscope) image and EDX (Energy Dispersive X-ray Spectroscopy) analysis were performed using a Tescan VGA3 instrument. Structural parameters were derived from N_2 adsorption-desorption isotherms using ASAP 2010 V5.00E. The pH_{PZC} (pH point of zero charge) of the adsorbent surface was identified using a series of solutions (0.01 M NaCl) with diverse pH levels (2.0 to 12.0). 50 mL of each solution was stirred for 12 hours after addition of 0.2 g of adsorbent. The final pH is measured and plotted against initial pH. The pH_{PZC}, where initial and final pH coincide, is determined from the plot [15].

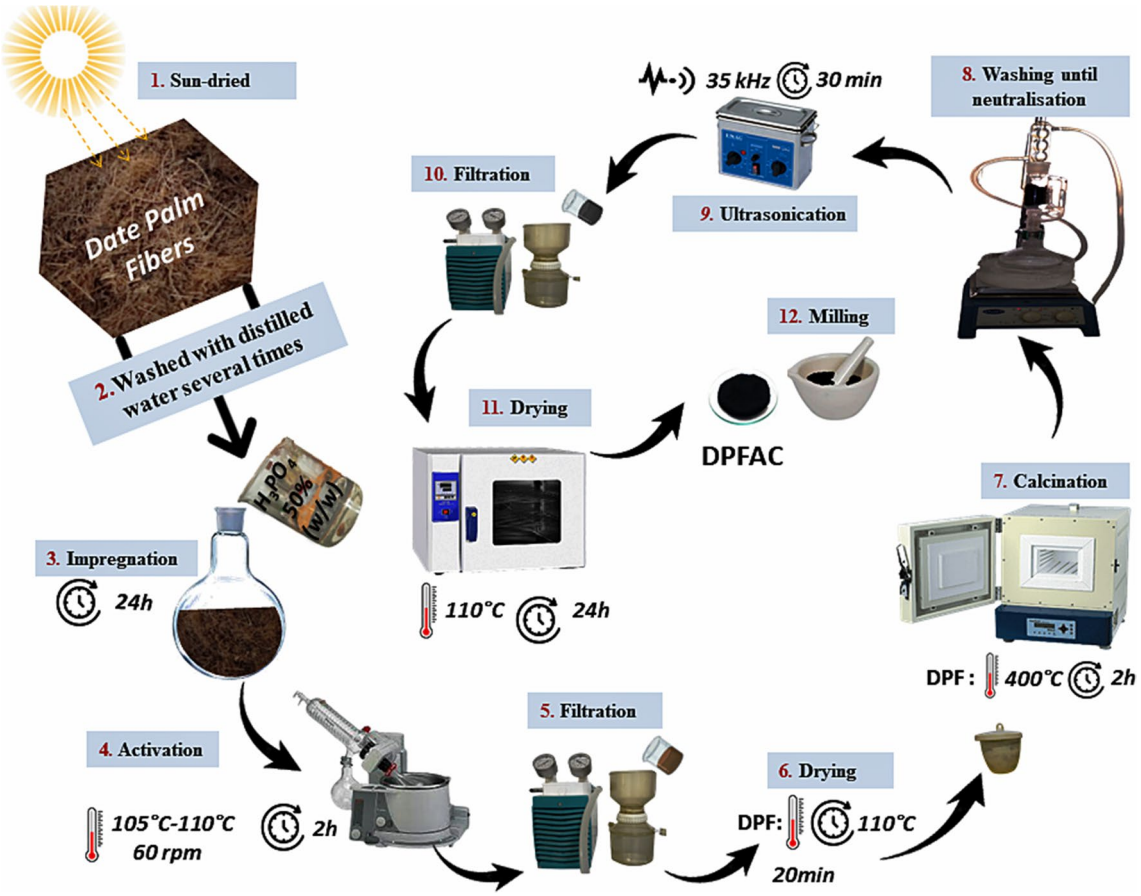

Fig. 1 Steps followed in the preparation of date palm fibers activated carbon (DPFAC)

2.4 Presentation of Adsorption Tests

Adsorption kinetic study was conducted under continuous magnetic stirring for durations ranging from 2 to 360 min. The treated solutions were prepared in 50 mL flasks, initially containing 10 mg/L Cu^{2+} and mixed with 4 g/L of DPFAC at an initial pH of 5.5 (pH of synthetic solution). Once the equilibrium time had been determined during the kinetic tests, the effect of initial Cu^{2+} content was studied in the range of 1 to 100 mg/L at 20 °C, and under an initial pH of around 5.5 with the addition of 4 g/L DPFAC. The data obtained is used to study the adsorption isotherms. To evaluate the impact of initial pH, the pH of the solutions (10 mg/L of Cu^{2+}) was adjusted between 2 and 12 using 0.1 M solutions of HCl and NaOH. Using solutions containing Cu^{2+} (10 mg/L) with the addition of DPFAC (4 g/L), the thermodynamic study was carried out simultaneously at temperatures in the range of 20 °C to 50 °C. Following each test, samples were filtered under vacuum. The residual content of Cu^{2+} ions in the solution was then measured through a PERKIN ELMER A700 atomic absorption spectrometer. To measure the pH of the solutions, a pH meter, model pH 7310P, was used.

3 Results and Discussion

3.1 Characterization Results of the Prepared Adsorbent

The analysis of FTIR spectrum of DPFAC sample (Fig. 2a) shows that the prepared adsorbent exhibits a variety of surface functional groups. -OH stretching vibration (3670—3550 cm^{-1}), C-H stretches of aliphatic groups (2900- 2850 cm^{-1}), C=O functional group in ketones, carboxylic acids and esters (1750–1600 cm^{-1}). Stretching of the aromatic ring C=C of benzene-like rings (1600–1550 cm^{-1}), C−O stretching in phenols, ethers, esters, acids, and alcohols (1200–1000 cm^{-1}). A similar report was also shown in [15, 37, 38]. The bands at 1200–1000 cm^{-1} are attributed to the characteristics of phosphor-carbonaceous compounds in DPFAC. According to Puziy et al., [39] and Alharbi et al. [23], the peaks in this region may be assigned to the stretching mode of P=O, P–O–C and P=OOH. These functional groups can contribute to the formation of bonds with copper ions.

Figure 2b shows the N_2 adsorption–desorption isotherms of DPFAC. Hysteresis appears at the pressure rate (P/P_0) between 0.4 and 0.8. According to Martins et al. [40] this hysteresis is related to the presence of mesopores in the material, which are associated with narrow slit-like pores and a small external surface area. Brunauer–Emmett–Teller (BET) analysis (Fig. 2b) indicated a well-developed pore structure with an average pore diameter of approximately 17.48 Å and a specific surface area of 834.79 m^2/g.

SEM image (Fig. 2c) confirmed the presence of a porous structure with well-developed pores and regular size and shape. The same finding was obtained by Alharbi et al. [23] after the H_3PO_4chemical treatment of leaf sheath date palm fibers. As suggested by Girgis and El-Hendawy [22], the pores in the activated carbon likely originate from the release of space previously occupied by phosphoric acid during carbonization. Additionally, ultrasonication is a process that enhances mass transfer [33]. Sound waves, consistent with the observations of Egbosiuba et al. [41], Suganya and Senthil-Kumar [42], and Hassan et al. [43], generate fluctuations in pressure within aqueous medium and can enhance chemical reactions, leading to the decomposition of water molecules into hydrogen and hydroxyl radicals. These radicals, in turn, generate a significant number of micro-bubbles that collapse in microseconds in the liquid-activated carbon, contributing to the overall porosity of the material. EDX analysis of DPFAC (Fig. 2c) indicated that it is rich in carbon (C) and oxygen (O) and their atomic percentages are: 82.80% and 16.28%, respectively. Gupta et al. [44] highlighted that biochars with high oxygen content have higher cation exchangeability.

3.2 Copper Removal Tests

3.2.1 Adsorption Kinetics Modeling

Results presented in Fig. 3 led to the following observations:

- The adsorption capacity of DPFAC towards Cu^{2+} ions increased with agitation time until a value of 2.437 mg/g was reached, corresponding to 97.47% efficiency.
- The equilibrium time for the process was 60 min.
- Beyond the equilibrium time, adsorption capacity decreases slightly.

The kinetic models described below (Eq. (1) [45], Eq. (2) [46], and Eq. (3) [47]) were adjusted to the experimental data to investigate the adsorption mechanisms of copper ions on DPFAC:

$$Pseudo-first-\mathrm{order}(PFO):\ q_t = q_e\left(1-e^{-k_1 t}\right) \quad (1)$$

$$Pseudo-second-\mathrm{order}(PSO):\ q_t = \frac{q_e^2 k_2 t}{1+q_e k_2 t} \quad (2)$$

$$Intra-particlediffusion:\ q_t = K_{int} t^{\frac{1}{2}} + Ci \quad (3)$$

In these equations, qe (mg/g) and qt (mg/g) represent the amounts of metal adsorbed at equilibrium and at time t (min), respectively. k_1 (min^{-1}) and k_2 (g/(mg.min)) denote the pseudo-first-order and pseudo-second-order rate

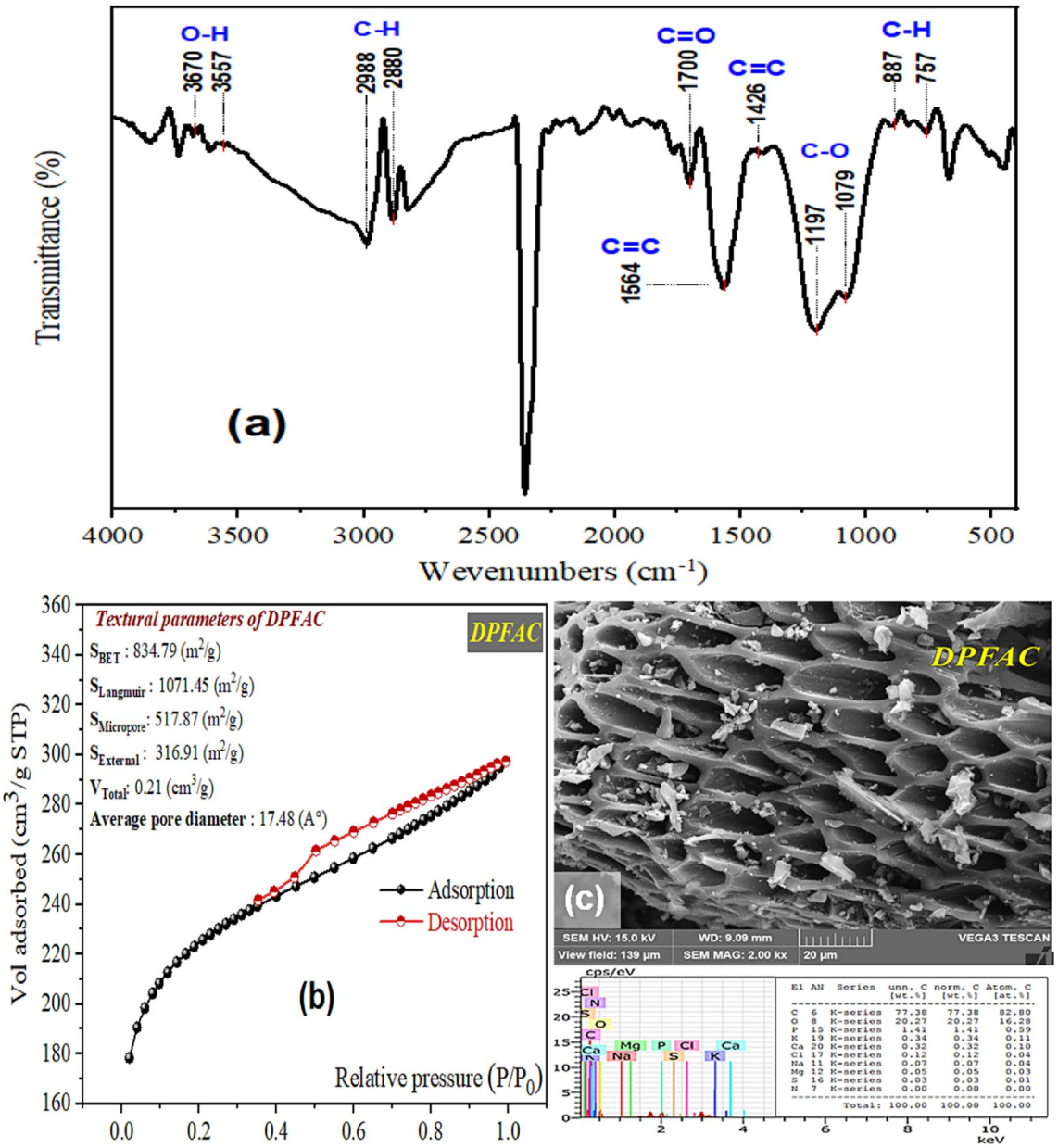

Fig. 2 **(a)** Analysis of functional groups based on the FTIR spectrum, **(b)**Results of N_2 adsorption–desorption isotherms, **(c)**SEM image and EDX analysis of DPFAC sample

constants, respectively. K_{int} (mg/g.min$^{1/2}$) and C_i (mg/g) represent the intra-particle diffusion model's constant and intercept, respectively.

As illustrated in Fig. 3a, the PSO curve exhibits a better fit to the experimental data compared to the PFO curve. This observation is further supported by the higher coefficient of determination (R^2) value and lower chi-square (χ^2) value associated with the PSO model (0.992; 5.835×10^{-5}) compared to the PFO model (0.822; 0.0014) (Table 1). Additionally, the adsorption capacity calculated using the PSO model ($q_{e2,cal}$) closely matches the experimentally determined adsorption capacity at equilibrium ($q_{e,exp}$). Based on the findings presented in Table 1, the following key observation can be drawn:

$$Cu^{2+}: q_{e1,cal}(PFO)(2.408\text{mg}/g) < q_{e2,cal}(PSO)(2.435\text{mg}/g) \approx q_{e,exp}(2.437\text{mg}/g)$$

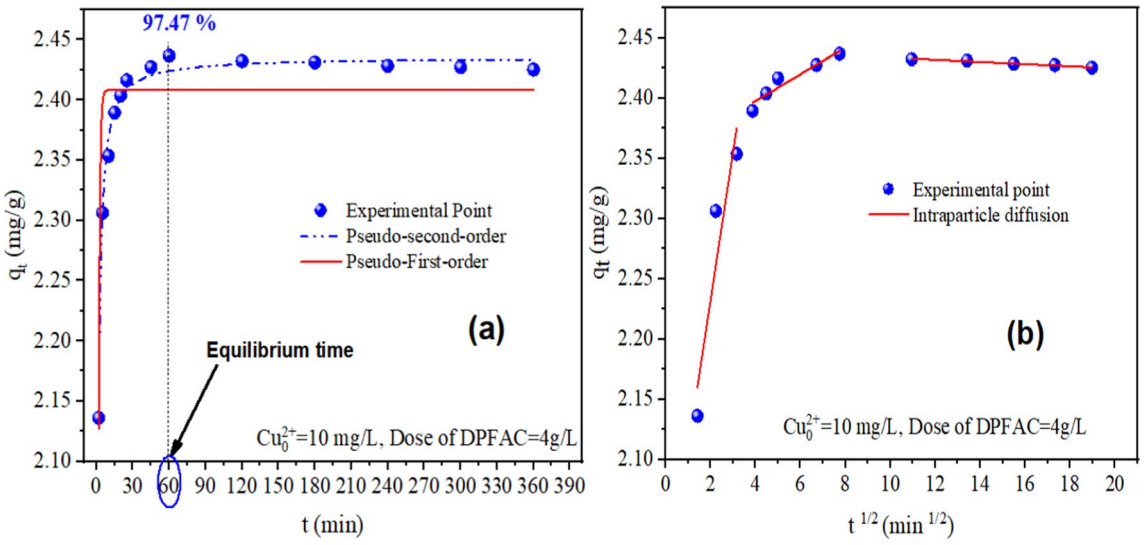

Fig. 3 **(a)** PFO, PSO and **(b)** Intraparticle diffusion models application to experimental points of copper ions adsorption kinetics on DPFAC

Table 1 Parameters of the PFO,PSO, and the intraparticle diffusion kinetics models for copper ions adsorption kinetic on DPFAC

Pseudo-First-order $q_t = q_e\left(1 - e^{-k_1 t}\right)$					Pseudo-second-order: $q_t = \frac{q_e^2 k_2 t}{1+q_e k_2 t}$			
$q_{e,exp}$ (mg/g)	$q_{el,cal}$ (mg/g)	k_1 (min^{-1})	R^2	χ^2	$q_{e\,2,cal}$ (mg/g)	k_2 (g/(mg.min))	R^2	χ^2
2.437	2.408	1.074	0.822	0.0014	2.435	1.456	0.992	5.835×10^{-5}
Intra-particle diffusion: $q_t = K_{int} t^{\frac{1}{2}} + Ci$								
$K_{int,1}$ (mg/g.$min^{1/2}$)	C_1 (mg/g)	R^2	$K_{int,2}$ (mg/g.$min^{1/2}$)	C_2 (mg/g)	R^2	$K_{int,3}$ (mg/g.$min^{1/2}$)	C_3 (mg/g)	R^2
0.123	1.986	0.883	0.0112	2.353	0.92	-8.913	2.442	0.967

The applicability of the PSO compared with the PFO suggests that the retention of copper ions onto the adsorbent is mainly chemical [48, 49].

To investigate the implication of intra-particle diffusion in the adsorption of copper ions onto the DPFAC surface, the intra-particle diffusion model was applied, plotting qt versus $t^{1/2}$ (Fig. 3a). As depicted in Fig. 3b, the model satisfactorily fitted the experimental data. According to Abdulkareem et al. [50], this finding indicates that pore filling contributed positively to the adsorption mechanism of metal ions. The intraparticle diffusion plots exhibit three distinct linear segments. As the first segment does not pass through the origin, this suggests that additional sorption mechanisms beyond intra-particle diffusion might be contributing to the adsorption process [51]. In addition, the intra-particle diffusion rate constants (Table 1) follow the order:

$$K_{int,1}(0.123) > K_{int,2}(0.0112) > K_{int,2}(-8.913)(mg/g.min^{1/2})$$

The high slope of the first line ($K_{int,1}$) compared to the second ($K_{int,2}$) and third ($K_{int,3}$) lines suggests that copper ions are rapidly transferred from the solution to the DPFAC surface at the early stages of the adsorption process. This rapid transfer is followed by a slower rate of adsorption as equilibrium is approached.

3.2.2 pH Effect

The results (Fig. 4a) demonstrate a significant increase in copper adsorption efficiency from 87.72% at pH 2 to 99.32% at pH 12. Under acidic conditions, the abundance of H^+ ions competes with Cu^{2+} ions for adsorption sites on the DPFAC surface. When the pH exceeds pH point of zero charge of DPFAC (pH_{PZC} = 4.47) (Fig. 4a, 4b), the adsorbent surface becomes negatively charged due to deprotonation of surface OH groups. This negative charge intensifies with increasing pH, promoting electrostatic attraction between the negatively

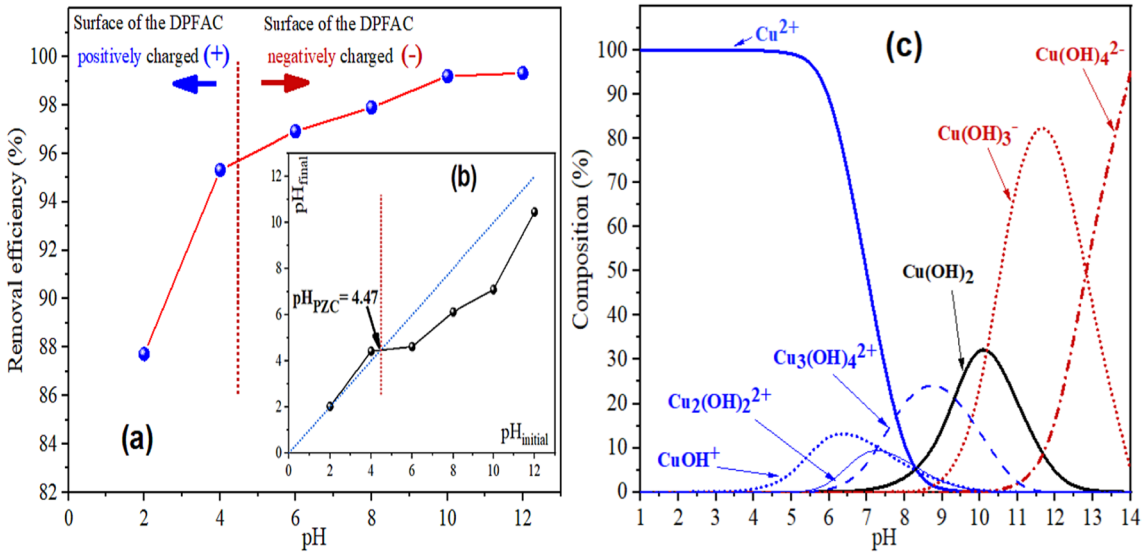

Fig. 4 **(a)** Efficiency of copper removal as a function of the initial pH of the solution (Cu_0^{2+}=10 mg/L, Dose de DPFAC = 4g/L, Contact time = 60 min). **(b)** DPFAC pH point of zero charge curve**. (c)**.Dominant copper species in an aqueous solution with Cu_0^{2+}=10 mg/L at different pH values and at 20°C using Visual MINTEQ software

charged adsorbent surface and the metal ions in solution, thereby enhancing adsorption efficiency [14, 52].

As evident from Fig. 4c, the Cu^{2+} species dominates the solution at pH values below 7, with minor contributions from $CuOH^+$, $Cu_2(OH)_2{}^{2+}$, and $Cu_2(OH)_4{}^{2+}$. Increasing the pH above 7 leads to the formation of anionic copper hydroxide species ($Cu(OH)_3{}^-$ and $Cu(OH)_4{}^{2-}$). The same approach was reported by Youcef et al. [52] and Soudani et al. [15]. Negatively charged species of copper have a low probability of adsorption on the DPFAC surface, which is negatively charged in this pH range. At this stage, the increase in copper ion removal efficiency is largely due to another mechanism other than adsorption, namely chemical precipitation in the solution in the form of $Cu(OH)_2$. In order to recover as many copper ions as possible on the surface of the DPFAC and avoid precipitation in the solution, it would be advisable to treat solutions with an initial pH of around 5.5.

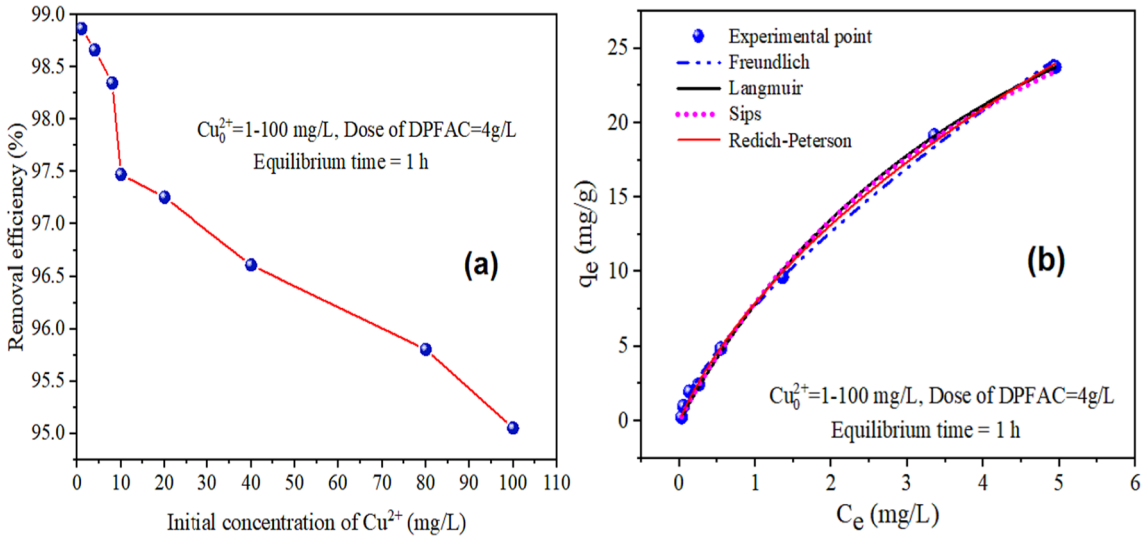

Fig. 5 Presentation of (**a**) Variation in removal efficiency as a function of variation in initial copper ions content (**b**) Adsorption isotherms of copper ions on DPFAC

3.2.3 Analysis of the Effect of Initial Concentration of Copper Ions and the Adsorption Isotherms

Results shown in Fig. 5a indicate that the removal efficiency of copper ions by adsorption on DPFAC decreases gradually from 97.20% to 95.05% with the increase in the initial concentration of Cu^{2+} from 1 mg/L to 100 mg/L, respectively. At low concentrations, copper ions had a large number of adsorption sites available. However, at higher concentrations, the adsorbent becomes saturated, reducing the number of sites available for further sorption. The same approach was advanced by Soudani et al. [15] and Vunain et al. [26].

The adsorption isotherm for copper on DPFAC was studied to define the adsorption process. An approach was developed to simulate the results obtained at the adsorption equilibrium by applying the following nonlinear isotherm models of Langmuir [53], Freundlich [54], Redlich–Peterson [55] and of Sips [56].The Eqs. (4) to (7) relating to these models are as follows:

$$Langmuir: q_e = \frac{Q_{max} K_L C_e}{1 + K_L C_e} \quad (4)$$

$$Freundlich: q_e = K_F C_e^{1/n} \quad (5)$$

$$Redlish - Peterson: q_e = \frac{K_{RP} C_e}{1 + a_{RP} C_e^{\beta}} \quad (6)$$

$$Sips: q_e = \frac{q_s K_s C_e^{1/nS}}{1 + Ks C_e^{1/nS}} \quad (7)$$

The parameters in these equations are defined as below:

q_e (mg/g) is the adsorption capacity of the adsorbent at equilibrium. Ce (mg/L) is the concentration of the adsorbate in solution at equilibrium.

Q_{max} (mg/g) is the maximum Langmuir adsorption capacity. K_L (L/mg) is the Langmuir equilibrium adsorption constant.

K_F ((mg/g)/(mg/L)$^{1/n}$) is the Freundlich constant. n (dimensionless) is the Freundlich factor.

K_{RP} (L/g) and a_{RP} (mg/L)$^{-\beta}$ are the constants of the Redlich-Peterson isotherm. β is the dimensionless Redlich-Peterson exponent, which must be between 0 and 1.

K_S (L /mg) is the Sips equilibrium constant. n_S (dimensionless) represents the heterogeneity of the adsorbent surface.

Equilibrium data for Cu^{2+} are presented using these four models in Fig. 5b. The parameters obtained by fitting each model are provided in Table 2.

Langmuir model, applied with a higher coefficient of determination ($R^2 > 0.99$) and a lower error value ($\chi^2 = 0.179$), showed the best consistency with the experimental data compared with the Freundlich, Sips and Redlich-Peterson models, respectively. This is an indication that the copper ions (Cu^{2+}) were adsorbed onto the homogeneous surface of the adsorbent forming a monolayer. The maximum Langmuir adsorption capacity $Q_{max}$is equal to 48.59 mg/g. By making a comparison with adsorbent prepared on the basis of date palm wasts [25, 33, 36, 57–60] (Table 3), it results that DPFAC is an adsorbent which has a sufficiently developed specific surface. In addition, it presented a satisfactory Langmuir adsorption capacity for the retention of copper in solution, compared to the adsorbents cited in Table 3.

By calculating the dimensionless parameter R_L, it can be checked whether the adsorption is favourable or not. This

Table 2 Parameters predicted by nonlinear isotherm models for copper ions adsorption on DPFAC

Langmuir: $q_e = \frac{Q_{max} K_L Ce}{1 + K_L Ce}$				Freundlich: $q_e = K_F C_e^{1/n}$			
K_L (L/mg)	Q_{max} (mg/g)	R^2	χ^2	K_F (mg/g)/(mg/L)$^{1/n}$	n	R^2	χ^2
0.193	48.587	0.998	0.179	7.739	1.399	0.998	0.207
Redlich-Peterson: $q_e = \frac{k_{Rp} C_e}{1 + a_{Rp} C_e^{\beta}}$				Sips: $q_e = \frac{q_s K_s C_e^{1/n_s}}{1 + K_s C_e^{1/n_s}}$			
K_{RP} (L/g)	a_{RP} (mg/L)$^{-\beta}$	β	R^2	χ^2	q_S (mg/g)	K_S (L /mg)	n_S	R^2	χ^2
13.316	0.677	0.593	0.998	0.153	48.721	0.195	1.024	0.998	0.213

Table 3 Results of copper ions adsorption on adsorbents prepared using date palms residues

Adsorbent	S_{BET} (m^2/g)	Q_{max} (mg/g)	Reference
Date palm fibers activated with H_3PO_4 (50%)	834.79	48.59	This study
Raw Date pits (Dried at 80 °C for 2 h)	n.a	7.40	[57]
Activated date pit using H_3PO_4 (85%)	n.a	33.44	
Date stones activated carbon using H_3PO_4 (60%)	826	31.25	[25]
Date palm trunk fiber, washed and dried at 105°C	n.a	25.25	[33]
Biochar of date palm wast biomass—Pyrolysis temperature of 800 °C	n.a	52.08	[58]
Date pits activated carbon with NaOH	377.6	194.4	[59]
Date palm fiber dried at 105^0Cfor 7 h	n.a	7.69	[60]
Date palm fiber activated with $ZnCl_2$	1603.50	25.05	[36]

S_{BET}: BET specific surface area, Q_{max}: maximal adsorption capacity of Langmuir isotherm, n.a: not available

parameter can be calculated by introducing the constant K_L obtained by adjusting the Langmuir isotherm to the experimental data. R_L is calculated as in Eq. (8) [48]:

$$R_L = \frac{1}{1+C_0K_L} \tag{8}$$

where: C_0 (mg/L) is the initial copper ion concentration, K_L(L/mg) is the Langmuir constant.

The isotherm is favourable when $0 < R_L < 1$, unfavorable for $R_L > 1$, and irreversible if $R_L = 0$. For copper solutions of 1 to 100 mg/L and for $K_L = 0.193$ L/mg, the following result is obtained:

$$0 < R_L(0.84 \text{ to } 0.05) < 1$$

From the results presented in Table 2, the values of 1/n of the Freundlich isotherm are lower than 1. According to the Freundlich theory [61, 62], when $1/n < 1$ pollutant adsorption is favourable on the adsorbent. The same theory has been attributed to a_{RP} ($a_{RP} < 1$) of the Redlich-Peterson model [62].

The Redlich-Peterson and Sips models are a combination of the Langmuir and Freundlich isotherms. The R^2 values are relatively satisfactory (close to 1) for both models, with a lower χ^2 value for the Sips model (Table 2).

3.2.4 Thermodynamic Study

The evolution of copper ions removal efficiency by adsorption on DPFAC (Fig. 6a) showed that increasing the solution

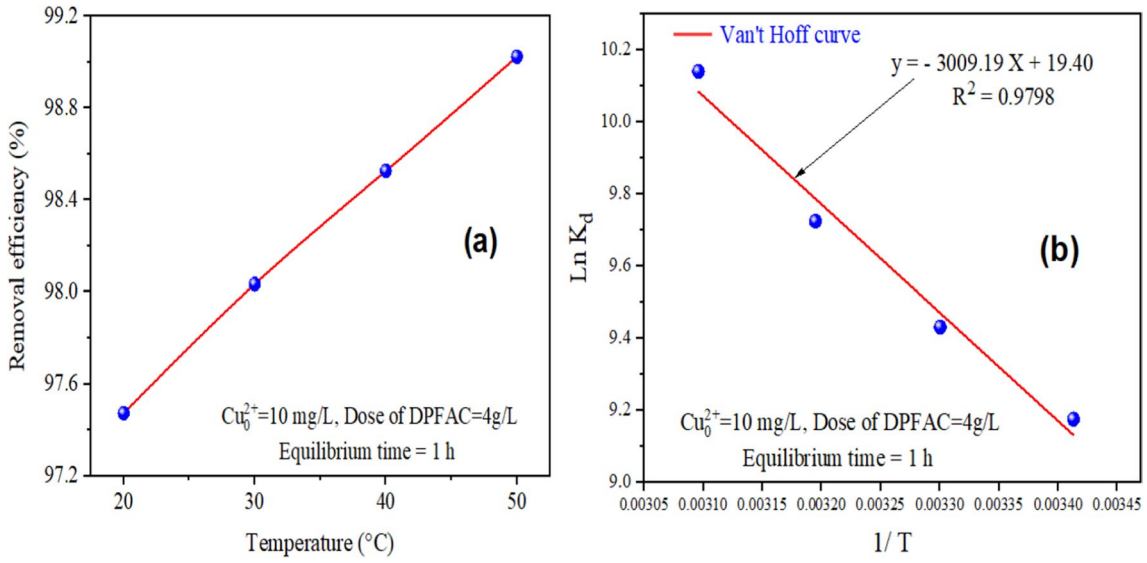

Fig. 6 Evolution of the removal efficiency (**a**), Van't Hoff curve (**b**) for copper ions adsorption on DPFAC according to temperature (T° = 20, 30, 40, 50 °C)

temperature improved slightly the treatment efficiency, from 97.47% at 20°C up to 99.02% at 50°C.

According to Abdulkareem et al. [50], the increase in temperature suggests enhancement of interaction between the metal ions and the adsorbent resulting in an increase of the kinetic energy and elevation of the mobility of the metal ions for increased diffusion to the surface of the adsorbent.

The data obtained were evaluated in terms of thermodynamic parameters, namely the standard Gibbs free energy (ΔG°), the variation in standard enthalpy (ΔH°) and the variation in entropy (ΔS°) [48, 63], which can be calculated according to the Eqs. (9) - (12):

$$\Delta G^{\circ} = \Delta H^{\circ} - T\Delta S^{\circ} \tag{9}$$

$$\Delta G^{\circ} = -RTLnK_d \tag{10}$$

where: R (8.314 J/mol.K) is the perfect gas constant of, T (Kelvin (K)) is the absolute temperature, K_d (dimensionless) is the distribution coefficient.

According to the approach of Biggar and Cheung [63], the distribution coefficient (K_d) is expressed in the formula below:

$$K_d = \frac{qe}{Ce} \tag{11}$$

As q_e is expressed in mg/g and Ce is given in mg/L, so K_d will be calculated in L/g.

By replacing the value ΔG° of Eq. (10) in Eq. (9) is obtained Eq. (12), that represents the Van't Hoff equation:

$$LnK_d = \frac{-\Delta H^{\circ}}{R} \times \frac{1}{T} + \frac{\Delta S^{\circ}}{R} \tag{12}$$

Canzano et al. [64] proposed that K_d (L/g) should be dimensionless by multiplying K_d (L/g) with 10^3.

ΔG° (J/mol) is calculated by Eq. (10). The intersection and the slope of the line LnK_d as a function of 1/T (Fig. 6b) are used to evaluate the entropy values (ΔS°) and enthalpy (ΔH°), respectively.

According to the results presented in the Table 4, the ΔG° values obtained are negative and increase in absolute values with increasing temperature, indicating favourable and more spontaneous adsorption with increasing temperature [15, 65]. Humelnicu et al. [65] have attributed this variation to the reduction in the thickness of the boundary layer surrounding the adsorbent, which rapidly facilitates the transfer of the pollutant to the surface of the adsorbent. The variation in enthalpy (ΔH°) is positive, supporting the hypothesis that the adsorption process is endothermic and bonding with copper ions at adsorbent sites are strong [66]. This provides evidence of the increase in copper ions removal efficiency with increasing temperature. In addition, achieving values of $\Delta H^{\circ} > 0$ indicates that physisorption may occur in addition to chemisorption at the surface of the adsorbent [67]. This effect is highlighted by the conclusions of the adsorption kinetics and isotherms tests. ΔS° values are > 0, suggesting an enhancement of randomness at the adsorbent/contaminant interface [15].

3.2.5 Overview of Copper Adsorption Mechanisms on DPFAC

Previous studies have reported that several functional groups present on the surface of activated carbon contribute to coordination with metal ions in solution [15, 49, 52, 67]. Based on the hypotheses advanced by these studies and the analysis of FTIR spectrum of DPFAC sample (Fig. 2), it can be stated that Cu-π bonds can be formed on the surface of DPFAC with aromatic C = O or C = C ligands. Copper ions or complex ions with alcoholic or phenolic hydroxyl (R-OH) and carboxyl (R-COOH) groups can also be formed.

Based on the results of the textural characterization of DPFAC, it was noted that the average diameter of its pores was of the order of 17.48 Å. Based on this effect, Copper has a low hydrated ionic radius (4.19 Å) [11, 68] which facilitates the pore-filling mechanism. In addition, the high adsorption efficiency obtained at equilibrium (97.47%) can be justified by the fact that copper has a high electronegativity (1.90) [15, 52, 69], which allows it to make surface chemical bonds easily. As mentioned above, the pH of the solution and the pH_{PZC} at the surface of the adsorbent affect these mechanisms. In the case of copper, it would be

Table 4 Parameters of copper ions adsorption thermodynamics on DPFAC (DPFAC dose = 4 g/L, $Cu^{2+}{}_0$ = 10 mg/L, T° = 20, 30, 40, 50 °C, Contact time = 60 min)

T (K)	Van't Hoff equation $LnK_d = \frac{-\Delta H^{\circ}}{R} \times \frac{1}{T} + \frac{\Delta S^{\circ}}{R}$	ΔG° (KJ/mol)	ΔH° (KJ/mol)	ΔS° (J/(K.mol))
293	Y = -3009.19x + 19.40	-22.348	25.018	161.292
303	R^2 = 0.9798	-23.758		
313		-25.305		
323		-27.232		

recommended to carry out the treatment in an acid medium (around 5) in order to avoid its precipitation in the solution in the form of $Cu(OH)_2$.

4 Conclusion

This study showed that activated carbon prepared from date palm fibers by using phosphoric acid (DPFAC) exhibited a well-developed morphology and texture. DPFAC presented varied surface bonds and a high specific surface area (834.79 m^2/g). In addition, the average pore diameter (17.48 Å) was large enough to receive copper ions with a hydrated ionic radius of 4.19 Å. All these parameters were favourable for the adsorption of Cu^{2+}.

Adsorption tests using DPFAC for copper ions removal in synthetic solutions achieved that the removal of copper ions is relatively fast, as the adsorption kinetics reached equilibrium within 60 min. At equilibrium time, the efficiency achieved was very satisfactory, at around 97.47%. The non-linear pseudo-second-order model provided a more accurate description of adsorption kinetics compared to the pseudo-first-order model. The process was influenced by the pH of the treatment and pH_{PZC} of the adsorbent, and the initial metal ions concentration in the solution. Based on these results, in order to improve the adsorption efficiency of Cu^{2+} on DPFAC and to avoid precipitation in the solution, it would be appropriate to treat the solutions with an initial pH of around 5.5. The isotherm models demonstrated an adequate fit to the experimental data, suggesting that copper ions removal by adsorption onto DPFAC was favourable. The Langmuir isotherm exhibited the closest agreement with the experimental data compared to the other tested models. The Langmuir Q_{max} reached 48.59 mg/g. Calculation of thermodynamic parameters confirmed that the adsorption process was spontaneous and endothermic, with a high degree of randomness on the surface of DPFAC. The predominant adsorption mechanisms for copper ions on DPFAC involve electrostatic attraction, pore filling, surface complexation, and Cu-π interactions. These considerations highlight the significant potential for DPFAC derived from date palm fibers to be improved as a suitable adsorbent for the removal of copper ions from wastewater.

Acknowledgements This study was performed at the LARHYSS Laboratory- University Mohamed Khider, Biskra-Algeria, and supported by the DGRSDT of the Ministry of Higher Education and Scientific Research-Algeria.

Funding No funds, grants, or other support was received.

Data Availability The data used to support this article appears in the article and in its online supplementary material.

Declarations

Competing Interest Authors have no competing interests to declare.

References

1. Ouakouak A, Youcef L (2016) Adsorption des ions Cu^{2+} sur un charbon actif en poudre et une bentonite sodique. LARHYSS J 27:39–61
2. Benalia MC, Youcef L, Bouaziz MG, Achour S, Menasra H (2022) Removal of heavy metals from industrial wastewater by chemical precipitation: mechanisms and sludge characterization. Arab J Sci Eng 47:5587–5599. https://doi.org/10.1007/s13369-021-05525-7
3. Bumajdad A, Hasila P (2023) Surface modification of date palm activated carbonaceous materials for heavy metal removal and CO_2 adsorption. Arab J Chem 16(1):104403. https://doi.org/10.1016/j.arabjc.2022.104403
4. Singh V, Singh N, Rai SN, Kumar A, Singh AK, Singh MP, Sahoo A, Shekhar S, Vamanu E, Mishra V (2023) Heavy Metal Contamination in the Aquatic Ecosystem: Toxicity and Its Remediation Using Eco-Friendly Approaches. Toxics 11(147):1–15. https://doi.org/10.3390/toxics11020147
5. Singh V, Singh N, Verma M, Kamal R, Tiwari R, Sanjay Chivate M, Rai SN, Kumar A, Singh A, Singh MP, Vamanu E, Mishra V (2022) Hexavalent-Chromium-Induced Oxidative Stress and the Protective Role of Antioxidants against Cellular Toxicity. Antioxidants 11(12), 2375:2–14. https://doi.org/10.3390/antiox11122375
6. WHO (2008) Guidelines for drinking-water quality, Third edition: Volume1-Recommendations incorporating the first and second addenda, Geneva. https://www.who.int/publications/i/item/9789241547611
7. JORA (Journal officiel de la république Algérienne) (2014) N °13, 7 Joumada El Aoula 1435 Correspondant au 09 Mars 2014. ANNEXE Paramètres de qualité de l'eau de consommation humaine. https://faolex.fao.org/docs/pdf/alg133820.pdf
8. Potelon JL, Zysman K (1998) Le guide des analyses de l'eau potable. Éd. La Lettre du Cadre Territorial, Voiron, France
9. Egbosiuba TC, Abdulkareem AS (2021) Highly efficient as-synthesized and oxidized multi-walled carbon nanotubes for copper (II) and zinc (II) ion adsorption in a batch and fixed-bed process. J Mater Res Technol 15:2848–2872. https://doi.org/10.1016/j.jmrt.2021.09.094
10. Wongkoblap A, Ngernyen Y, Budsaereechai S, Charoenbood A (2013) Heavy metal removal from aqueous solution by using bentonite clay and activated carbon. In: Chemeca 2013: Challenging tomorrow. Engineers Australia, pp 689–694. https://search.informit.org/doi/10.3316/informit.9781922107077
11. Egbosiuba TC, Egwunyenga M C, Tijani JO, Mustapha S, Abdulkareem AS, Kovo AS, Krikstolaityte V, Veksha A, Wagner M, Lisak G (2022) Activated multi-walled carbon nanotubes decorated with zero valent nickel nanoparticles for arsenic, cadmium and lead adsorption from wastewater in a batch and continuous flow modes. J Hazard Mater 423, Part B, 126993. https://doi.org/10.1016/j.jhazmat.2021.126993
12. Krstić V, Urošević T, Pešovski B (2018) A review on adsorbents for treatment of water and wastewaters containing copper ions. Chem Eng Sci 192:273–287. https://doi.org/10.1016/j.ces.2018.07.022
13. Raninga M, Mudgal A, Patel V K, Patel J, Sinha MK (2023)Modification of activated carbon-based adsorbent for removal of industrial

dyes and heavy metals: A review. Materials Today : Proc 77(Part 1): 286–294. https://doi.org/10.1016/j.matpr.2022.11.358
14. Esfandiar N, Suri R, McKenzie ER (2022) Competitive sorption of Cd, Cr, Cu, Ni, Pb and Zn from stormwater runoff by five low-cost sorbents; Effects of co-contaminants, humic acid, salinity and pH. J Hazard Mater 423(Part A):126938. https://doi.org/10.1016/j.jhazmat.2021.126938
15. Soudani A, Youcef L, Bulgariu L, Youcef S, Toumi K, Soudani N (2022) Characterizing and modeling of Oak fruit shells biochar as an adsorbent for the removal of Cu, Cd, and Zn in single and in competitive systems. Chem Eng Res Des 188:972–987. https://doi.org/10.1016/j.cherd.2022.10.009
16. Wang B, Lan J, Bo Ch, Gong B, Ou J (2023) Adsorption of heavy metal onto biomass-derived activated carbon: review. RSC Adv 13(7):4275–4302. https://doi.org/10.1039/D2RA07911A
17. Peng H, Gao P, Chu G, Pan B, Peng J, Xing B (2017) Enhanced adsorption of Cu(II) and Cd(II) by phosphoric acid-modified biochars. Environ Pollut 229:846–853. https://doi.org/10.1016/j.envpol.2017.07.004
18. Choi SS, Tae Ryeong ChoiTR, Choi HJ (2021) Surface Modification of Phosphoric Acid-activated Carbon in Spent Coffee Grounds to Enhance Cu(II) Adsorption from Aqueous Solutions. Appl Chem Eng 32(5) : 589–598. https://doi.org/10.14478/ace.2021.1074
19. Reddy KSK, Al Shoaibi A, Srinivasakannan C (2012) A comparison of microstructure and adsorption characteristics of activated carbons by CO_2 and H_3PO_4 activation from date palm pits. New Carbon Mater 27(5):344–351. https://doi.org/10.1016/S1872-5805(12)60020-1
20. Dechapanya W, Khamwichit A (2023) Biosorption of aqueous Pb(II) by H_3PO_4-activated biochar prepared from palm kernel shells (PKS). Heliyon 9(7):e17250. https://doi.org/10.1016/j.heliyon.2023.e17250
21. Alhawtali S, El-Harbawi M, El Blidi L, Alrashed MM, Alzobidi A, Yin CY (2024) Date Palm Leaflet-Derived Carbon Microspheres Activated Using Phosphoric Acid for Efficient Lead (II) Adsorption. C 10(26). https://doi.org/10.3390/c10010026
22. Girgis BS, El-Hendawy ANA (2002) Porosity development in activated carbons obtained from date pits under chemical activation with phosphoric acid. Microporous Mesoporous Mater 52(2):105–117. https://doi.org/10.1016/s1387-1811(01)00481-4
23. Alharbi HA, Hameed BH, Alotaibi KD, Aloud SS, Al-Modaihsh AS (2022) Mesoporous Activated carbon from Leaf Sheath Date Palm Fibers by Microwave-Assisted Phosphoric Acid Activation for efficient Dye Adsorption. ACS Omega 7(50):46079–46089. https://doi.org/10.1021/acsomega.2c03755
24. Jibril B, Houache O, Al-Maamari R, Badir Al-Rashidi B (2008) Effects of H_3PO_4 and KOH in carbonization of lignocellulosic material. J Anal Appl Pyrolysis 83(2):151–156. https://doi.org/10.1016/j.jaap.2008.07.003
25. Bouhamed F, Elouear Z, Bouzid J (2012) Adsorptive removal of copper (II) from aqueous solutions on activated carbon prepared from Tunisian date stones: Equilibrium, kinetics and thermodynamics. J Taiwan Inst Chem 43(5):741–749. https://doi.org/10.1016/j.jtice.2012.02.011
26. Vunain E, Kenneth D, Biswick T (2017) Synthesis and characterization of low-cost activated carbon prepared from Malawian baobab fruit shells by H_3PO_4 activation for removal of Cu (II) ions: equilibrium and kinetics studies. Appl Water Sci 7:4301–4319. https://doi.org/10.1007/s13201-017-0573-x
27. Bastidas-Oyanedel J-R, Fang C, Almardeai S, Javid U, Yousuf A, Schmidt JE (2016) Waste biorefinery in arid/semi-arid regions. Bioresour Technol 215:21–28. https://doi.org/10.1016/j.biortech.2016.04.010
28. Rekis A (2021) Conservation des ressources phytogénétiques en Algérie : cas des palmiers dattiers cultivés et sub-spontanés (Phoenixdactylifera L.). Thèse de doctorat en science agronomique. Université Mohamed Khider Biskra. Algérie. http://thesis.univ-biskra.dz/5485/
29. AL-Oqla FM, Alothman OY, Jawaid M, Sapuan S, Es-Saheb MH (2014) Processing and properties of date palm fibers and its composites. BiomassBioenergy: Process Prop 1–25.https://doi.org/10.1007/978-3-319-07641-6_1
30. Al Arni S, Elwaheidi M, Converti A, Benaissa M, Salih AAM, Ghareba S (2022) Abbas N (2022) Application of Date Palm Surface Fiber as an Efficient Biosorbent for Wastewater Treatment. Chem Bio Eng Reviews 10(1):1–11. https://doi.org/10.1002/cben.202200008
31. Shafiq M, Alazba AA, Amin MT (2018) Removal of heavy metals from wastewater using date palm as a biosorbent: a comparative review. Sains Malays 47(1):35–49. https://doi.org/10.17576/jsm-2018-4701-05
32. Al-Ghamdi A, Altaher H, Omar W (2013) Application of date palm trunk fibers as adsorbents for removal of Cd^{+2} ions from aqueous solution. J Water Reuse Desalination 03(1):47–54. https://doi.org/10.2166/wrd.2013.031
33. Amin MT, Alazba AA, Shafiq M (2016) Adsorption of copper (Cu^{2+}) from aqueous solution using date palm trunk fibre: isotherms and kinetics. Desalination Water Treat 57(47):22454–22466. https://doi.org/10.1080/19443994.2015.1131635
34. Hikmat NA, Qassim BB, Khethi MT (2014) Thermodynamic and kinetic studies of lead adsorption from aquesous solution onto petiole and fiber of palm tree. Am J Chem 4(4):116–124. https://doi.org/10.5923/j.chemistry.20140404.02
35. Basheer AO, Hanafiah MM, Alsaadi MA, Al-Douri Y, Al-Raad AA (2021) Synthesis and optimization of high surface area mesoporous date palm fiber-based nanostructured powder activated carbon for aluminum removal. Chin J Chem Eng 32:472–484. https://doi.org/10.1016/j.cjche.2020.09.071
36. Melliti A, Yılmaz M, Sillanpää M, Hamrouni B, Vurm R (2023) Low-cost date palm fiber activated carbon for effective and fast heavy metal adsorption from water: Characterization, equilibrium, and kinetics studies. Colloids Surf A Physicochem Eng Asp 672:131775. https://doi.org/10.1016/j.colsurfa.2023.131775
37. Mohan D, Singh KP (2002) Single- and multi-component adsorption of cadmium and zinc using activated carbon derived from bagasse-an agricultural waste. Water Res 36:2304–2318. https://doi.org/10.1016/s0043-1354(01)00447-x
38. Adibmehr M, Faghihian H (2018) Magnetization and functionalization of activated carbon prepared by oak shell biowaste for removal of Pb^{2+} from aqueous solutions. Chem Eng Commun 205:519–532. https://doi.org/10.1080/00986445.2017.1404461
39. Puziy AM, Poddubnaya OI, Martínez-Alonso A, Castro-Muñiz A, Suárez-García F, Tascón JMD (2007) Oxygen and phosphorus enriched carbons from lignocellulosic material. Carbon 45:1941–1950. https://doi.org/10.1016/j.carbon.2007.06.014
40. Martins AC, Pezoti O, Cazetta AL, Bedin KC, Yamazaki DAS, Bandoch GFG, Asefa T, Visentainer JV, Almeida VC (2015) Removal of tetracycline by NaOH-activated carbon produced from macadamia nut shells: Kinetic and equilibrium studies. Chem Eng J 260:291–299. https://doi.org/10.1016/j.cej.2014.09.017
41. Egbosiuba TC, Abdulkareem AS, Kovo AS, Afolabi EA, Tijani JO, Auta M, Roos WD (2020) Ultrasonic enhanced adsorption of methylene blue onto the optimized surface area of activated carbon: Adsorption isotherm, kinetics and thermodynamics. Chem Eng Res Des 15:315–336. https://doi.org/10.1016/j.cherd.2019.10.016
42. Suganya S, Senthil Kumar PS (2018) Influence of ultrasonic waves on preparation of active carbon from coffee waste for the reclamation of effluents containing Cr(VI) ions. J IndEngChem 60:418–430. https://doi.org/10.1016/j.jiec.2017.11.029

43. Hassan MR, Yakout SM, Abdeltawab AA, Aly MI (2021) Ultrasound facilitates and improves removal of triphenylmethane (crystal violet) dye from aqueous solution by activated charcoal: A kinetic study. J SaudiChem Soc 25(6):10123. https://doi.org/10.1016/j.jscs.2021.101231
44. Gupta S, Sireesha S, Sreedhar I, Patel CM, Anitha KL (2020) Latest trends in heavy metal removal from wastewater by biochar based sorbents. J Water Process Eng 38:101561. https://doi.org/10.1016/j.jwpe.2020.101561
45. Ho YS, Mckay G (1998) Comparison of chemisorption kinetic models applied to pollutant removal on various sorbents. Process Saf Environ Prot 76(4):332–340. https://doi.org/10.1205/095758298529696
46. Lagergren SK (1898) About the theory of so-called adsorption of soluble substances. Sven Vetenskapsakad Handingarl 24:1–39
47. Weber WJ, Morris JC (1963) Kinetics of adsorption on carbon from solution. Sanit Eng Div, ASCE 89(2):31–60. https://doi.org/10.1061/jsedai.0000430
48. Tran HN, You SJ, Hosseini BA, Chao HP (2017) Mistakes and inconsistencies regarding adsorption of contaminants from aqueous solutions: A critical review. Water Res 120(1):88–116. https://doi.org/10.1016/j.watres.2017.04.014
49. Uko CA, Tijani JO, Abdulkareem SA, Mustapha S, Egbosiuba TC, Muzenda E (2022) Adsorptive properties of MgO/WO3 nanoadsorbent for selected heavy metals removal from indigenous dyeing wastewater. Process Saf Environ Prot 162:775–794. https://doi.org/10.1016/j.psep.2022.04.057
50. Abdulkareem AS, Hamzat WA, Tijani JO, Egbosiuba TCh, Mustapha S, Abubakre OK, Okafor BO, Babayemi AK (2023) Isotherm, kinetics, thermodynamics and mechanism of metal ions adsorption from electroplating wastewater using treated and functionalized carbon nanotubes. J Environ Chem Eng 11(1):109180. https://doi.org/10.1016/j.jece.2022.109180
51. Cruz-Lopes L, Macena M, Esteves B, Santos-Vieira I (2022) Lignocellulosic Materials Used as Biosorbents for the Capture of Nickel (II) in Aqueous Solution. Appl Sci 12(2):933. https://doi.org/10.3390/app12020933
52. Youcef S, Guergazi S, Youcef L (2022) Adsorption modeling of Cu and Zn in single and combined systems onto activated carbon of olive stone. Modeling Earth Sys Environ 8:3927–3940. https://doi.org/10.1007/s40808-021-01335-w
53. Langmuir I (1916) The constitution and fundamental properties of solids and liquids. J Am Chem Soc 38(11):2221–2295. https://doi.org/10.1021/ja02268a002
54. Freundlich HMF (1906) Über die Adsorption in Lösungen. Zeitschriftfür Physikalische Chemie 57(1):385–470. https://doi.org/10.1515/zpch-1907-5723
55. Redlich O, Peterson DL (1959) A useful adsorption isotherm. J Phys Chem 63(6):1024. https://doi.org/10.1021/j150576a611
56. Sips R J (1948) On the structure of a catalyst surface. J Chem Phys 16:490–495.https://doi.org/10.1063/1.1746922
57. Hilal NM, Ahmed IA, El-Sayed RE (2012) Activated and non-activated date pits adsorbents for the removal of Copper (II) and Cadmium (II) from aqueous solutions. ISRN Phys Chem 985853.https://doi.org/10.5402/2012/985853
58. Amin MT, Alazba AA, Shafiq M (2019) Application of biochar derived from date palm biomass for removal of lead and copper ions in a batch reactor: kinetics and isotherm scrutiny. Chem Phys Lett 722:64–73. https://doi.org/10.1016/j.cplett.2019.02.018
59. Aldawsari A, Khan MA, Hameed BH, Alqadami AA, Siddiqui MR, Alothman ZA, Hadj Ahmed AYB (2017) Mercerized mesoporous date pit activated carbon-A novel adsorbent to sequester potentially toxic divalent heavy metals from water. PLoS ONE 12(9):e0184493. https://doi.org/10.1371/journal.pone.0184493
60. Saravanan AM, Al Hashmi RA, Jesil A, Achuthan M, Walke S, Al Rashdi S, Al Balushi N, Jahan S (2022) Experimental scrutinization on the treatment of synthetic wastewater using neem bark and date palm fiber as an adsorbent. Rasayan J Chem Special Issue 204–215. https://doi.org/10.31788/RJC.2022.1558134
61. Günay A, Ersoy B, Dikmen S, Evcin A (2013) Investigation of equilibrium, kinetic, thermodynamic and mechanism of Basic Blue 16 adsorption by montmorillonitic clay. Adsorption 19:757–768. https://doi.org/10.1007/s10450-013-9509-4
62. Amer MW, Awwad AM (2017) Removal of Zn(II), Cd(II) and Cu(II) Ions from Aqueous Solution by Nano-Structured Kaolinite. Asian J Chem 29(5):965–969. https://doi.org/10.14233/ajchem.2017.20343
63. Biggar JW, Cheung MW (1973) Adsorption of picloram (4-amino-3,5,6 trichloropicolinic acid) on panoche, ephrata, and palouse soils: a thermodynamic approach to the adsorption mechanism1. SoilSci Soc Am J 37(6):863–868. https://doi.org/10.2136/sssaj1973.03615995003700060022x
64. Canzano S, Pasquale I, Stefano S, Sante C (2012) Comment on "Removal of anionic dye Congo red from aqueous solution by raw pine and acid-treated pine cone powder as adsorbent: Equilibrium, thermodynamic, kinetics, mechanism and process design." Water Res 46(13):4314–4315. https://doi.org/10.1016/j.watres.2012.05.040
65. Humelnicu D, Ignat M, Doroftei F (2015) Agricultural by-products as low-cost sorbents for the removal of heavy metals from dilute wastewaters. Environ Monit Assess 187:1–11. https://doi.org/10.1007/s10661-015-4454-1
66. Zahaf F, Marouf R, Ouadjenia F, Schott J (2018) Kinetic and thermodynamic studies of the adsorption of Pb (II), Cr (III) and Cu (II) onto modified bentonite. Desal Water Treat 131:282–290.https://doi.org/10.5004/dwt.2018.23060
67. Cantu Y, Remes A, Reyna A, Martinez D, Villarreal J, Ramos H, Trevino S, Tamez C, Martinez A, Eubanks T, Parsons JG (2014) Thermodynamics, Kinetics, and Activation energy Studies of the sorption of chromium(III) and chromium(VI) to a Mn_3O_4 nanomaterial. Chem Eng J 254:374–383. https://doi.org/10.1016/j.cej.2014.05.110
68. Pelalak R, Heidari Z, Khatami SM, Kurniawan TA, Marjani A, Shirazian S (2021) Oak wood ash/GO/Fe_3O_4 adsorption efficiencies for cadmium and lead removal from aqueous solution: Kinetics, equilibrium and thermodynamic evaluation. Arab J Chem 14(3):102991. https://doi.org/10.1016/j.arabjc.2021.102991
69. Loganathan P, Shim WG, Sounthararajah DP, Kalaruban MNur T, Vigneswaran S (2018) Modelling equilibrium adsorption of single, binary, and ternary combinations of Cu, Pb, and Zn onto granular activated carbon. Environ Sci Pollut Res 25:6664–6675(2018). https://doi.org/10.1007/s11356-018-1793-9